

Large variations in the hole spin splitting of quantum-wire subband edges

D. Csontos¹ and U. Zülicke^{1,2}

¹*Institute of Fundamental Sciences, Massey University, Private Bag 11 222, Palmerston North, New Zealand*

²*MacDiarmid Institute for Advanced Materials and Nanotechnology, Massey University, Palmerston North, New Zealand*

(Dated: May 19, 2018)

We study Zeeman splitting of zone-center subband edges in a cylindrical hole wire subject to a magnetic field parallel to its axis. The g -factor turns out to fluctuate strongly as a function of wire-subband index, assuming values that differ substantially from those found in higher-dimensional systems. We analyze the spin properties of hole-wire states using invariants of the spin-3/2 density matrix and find a strong correlation between g -factor value and the profile of hole-spin polarization density. Our results suggest possibilities for confinement engineering of hole spin splittings.

PACS numbers: 73.21.Hb, 72.25.Dc, 71.70.Ej

Spin splitting of charge carriers in semiconductors has been a focus of recent research interest, partly because it may form the basis for the new paradigms of spin-based electronics and quantum information processing.¹ Besides such possible applications, intriguing fundamental-science questions motivate the study of charge carriers' spin properties. In particular, the quantum-mechanical coupling between spin and orbital degrees of freedom enables a host of, sometimes counterintuitive, mechanisms for manipulating spins in nanostructures.² As states in the valence band of a typical semiconductor are subject to a strong spin-orbit coupling, hole spin splittings will be highly tunable by geometrical and quantum-confinement effects. Large anisotropies of hole g -factors in quantum wells,³ point contacts,⁴ quantum dots,⁵ and localized acceptor states⁶ provide pertinent examples. The origin of such peculiar hole-spin properties can be traced to the fact that quasiparticles from the top-most valence band are characterized by total angular momentum (spin) 3/2. (Conduction-band electrons are spin-1/2 particles like electrons in vacuum.) Although spin is an intrinsically quantum degree of freedom, it has been possible to rationalize spin-1/2 physics largely in terms of a magnetic-dipole analogy. This classical-physics-inspired vehicle for our understanding succeeds because any spin-1/2 density matrix is fully characterized⁷ by the (trivial) particle density and a dipole moment associated with spin-polarization. In contrast, the spin-3/2 density matrix has two more invariants, a quadrupole and an octupole moment.⁸ As a surprising implication, magnetic fields do not always induce a spin polarization in two-dimensional (2D) hole systems.⁹

Our theoretical study presented here reveals the drastic influence of a quantum-wire confinement on spin-3/2 physics. Figure 1 shows universal results for the Landé g -factors of low-lying subband edges in cylindrical quantum wires subject to a parallel magnetic field. Two surprising features are apparent. First, g^* is seen to assume unusual values. Considering the wire axis to be a natural quantization axis for hole spin and remembering that spin-3/2 projection eigenvalues are $\pm 3/2$ and $\pm 1/2$, we would expect to find only 6κ and 2κ as possible g -factors. (Here κ is the hole g -factor in the bulk material).¹⁰ In Fig. 1, quite different numbers are found. Second, a strong variation of g -factor values between different subbands is observed. These features contrast also with situations found in 2D hole systems where confinement results in the suppression

of field-induced spin polarization³ and g -factors close to 0 and 4κ emerge.^{11,12,13}

In the following, we show how the anomalous behavior of wire-subband spin splittings is rooted in peculiar patterns of hole-spin dipole density that arise from the interplay between quasi-onedimensional (1D) confinement and spin-orbit coupling in the valence band. Our results are experimentally testable, as Zeeman splitting of quasi-1D subband edges can be measured directly in transport experiments.¹⁴ P-type versions of recently fabricated highly symmetric semiconductor nanowires¹⁵ should be particularly well-suited for observing effects discussed in this work. Our study is also relevant for understanding spin properties of quasi-1D hole systems realized in 2D semiconductor heterostructures^{4,16,17} and provides physical insight for the interpretation of recent numerical results.^{18,19,20}

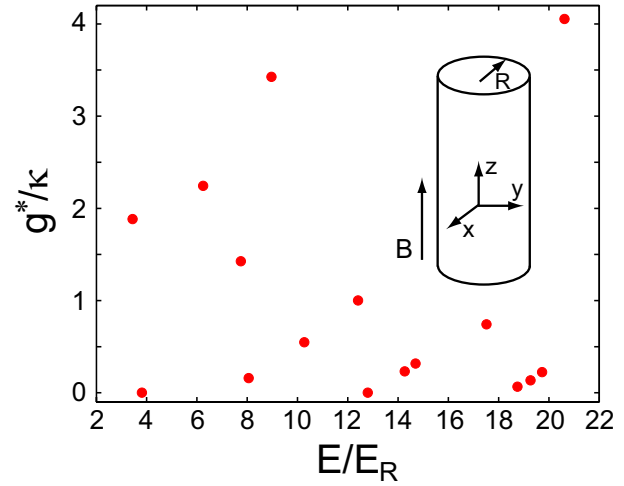


FIG. 1: (Color online) Landé factors g^* of low-lying subband edges in a cylindrical hole quantum wire (in units of the bulk hole g -factor κ). The abscissa shows subband energies measured from the valence-band top in units of $E_R = -\gamma_1 \hbar^2 / (2m_0 R^2)$. γ_1 is a materials-dependent (Luttinger) parameter, m_0 the electron mass in vacuum, and R the wire radius. The calculation is based on the spherical Luttinger model¹⁰ for the top valence band and assumed the GaAs value (0.37) for the relative spin-orbit coupling strength γ_s/γ_1 .

The remainder of this article is organized as follows. We first describe the theoretical formalism for calculating hole-wire subband energies and g -factors. After that, the characterization of spin-3/2 density matrices in terms of multipole invariants is introduced and results for the cylindrical-wire subband edges are presented. The emerging correlation between hole spin-dipole density and g -factor will be discussed. In closing, we comment on the effect of deviations from certain idealities assumed in our theoretical description.

Cylindrical hole quantum wire in a parallel magnetic field. We adopt the Luttinger model¹⁰ to describe states in the top-most valence band of a bulk semiconductor. The corresponding Hamiltonian operates in the 4×4 space spanned by eigenstates of spin-3/2 projection on an arbitrary axis with quantum numbers $\pm 3/2$ (heavy holes, HH) and $\pm 1/2$ (light holes, LH). It reads in the spherical approximation^{10,21}

$$\mathcal{H}_L = -\frac{\gamma_1}{2m_0} p^2 + \frac{\gamma_s}{m_0} \left[\left(\mathbf{p} \cdot \hat{\mathbf{J}} \right)^2 - \frac{5}{4} p^2 \mathbf{1}_{4 \times 4} \right] . \quad (1)$$

We denote linear orbital hole momentum by \mathbf{p} , $\hat{\mathbf{J}}$ is the vector of spin-3/2 matrixes, and m_0 the vacuum electron mass. Energies are measured from the valence-band edge. The ratio $\bar{\gamma} \equiv \gamma_s/\gamma_1$ of Luttinger band-structure parameters quantifies the relative strength of spin-orbit coupling in the valence band.

We consider a wire that is parallel to the z axis and subject to Zeeman splitting due to a magnetic field pointing in the same direction. Thus it is useful to choose the representation where \hat{J}_z is diagonal. As we are focused on finding hole-wire subband edges at the zone center,²² we set $p_z = 0$. Orbital magnetic-field effects are neglected.²³ To determine bulk hole states that can be superimposed to find cylindrical-wire subband states, we use polar coordinates r , φ and the wave-function *ansatz*²⁴

$$\psi(r, \varphi) = e^{im\varphi} \begin{pmatrix} a_m J_m(kr) \\ e^{i\varphi} b_m J_{m+1}(kr) \\ e^{2i\varphi} c_m J_{m+2}(kr) \\ e^{3i\varphi} d_m J_{m+3}(kr) \end{pmatrix} . \quad (2)$$

$J_m(x)$ is a Bessel function, and a_m, \dots, d_m are constants. Uniqueness of the hole wave function requires m to be an integer. Inserting Eq. (2) into the stationary Schrödinger equation simplifies the Hamiltonian for hole motion transverse to the z axis, which now reads²⁴

$$\mathcal{H}_L^{(\perp)} = -\frac{\gamma_1 \hbar^2 k^2}{2m_0} \left\{ \mathbf{1}_{4 \times 4} + \bar{\gamma} \left[\hat{J}_z^2 - \frac{5}{4} \mathbf{1}_{4 \times 4} + \hat{J}_+^2 + \hat{J}_-^2 \right] \right\} . \quad (3)$$

Here $\hat{J}_{\pm} = (\hat{J}_x \pm i\hat{J}_y)/\sqrt{2}$ are ladder operators for the z -axis projection of spin.

Zeeman splitting due to a magnetic field with magnitude B applied parallel to the z axis is described by $\mathcal{H}_Z = 2\kappa\mu_B B \hat{J}_z$, which needs to be added to Eqs. (1) and (3). μ_B is the Bohr magneton, κ the bulk hole g -factor, and we neglected the small anisotropic part of Zeeman splitting in the bulk valence band.

Diagonalization of $\mathcal{H}_L^{(\perp)} + \mathcal{H}_Z$ yields bulk-hole eigenstates

that can be superimposed to find wire-subband bound states:

$$\psi_{km\alpha+}(r) = (a_{\alpha+} J_m(kr), 0, J_{m+2}(kr), 0)^T, \quad (4a)$$

$$\psi_{km\alpha-}(r) = (0, J_{-m-2}(kr), 0, a_{\alpha-} J_{-m}(kr))^T . \quad (4b)$$

We omit the polar-angle (φ)-dependent part since the wire potential is cylindrically symmetric. In Eq. (4), $\alpha = \pm 1$ labels eigenstates within subspaces spanned by HH and LH basis states having spin projection $\pm 3/2$ and $\mp 1/2$ (for $\psi_{km\alpha\pm}$, respectively). The coefficients $a_{\alpha\sigma}$ are given by

$$a_{\alpha\sigma} = \frac{1}{\sqrt{3}} \left[1 - 2\alpha \sqrt{1 + \zeta_{k\sigma} + \zeta_{k\sigma}^2} + 2\zeta_{k\sigma} \right], \quad (5)$$

where we used the abbreviation $\zeta_{k\sigma} = \sigma \kappa e B / (\gamma_s \hbar k^2)$, and $-e$ is the electron charge. The corresponding eigenenergies are, like the $a_{\alpha\sigma}$, independent of orbital angular momentum quantum number m :

$$E_{\alpha\sigma}(k) = -\frac{\gamma_1 \hbar^2 k^2}{2m_0} \left[1 - 2\alpha \bar{\gamma} \sqrt{1 + \zeta_{k\sigma} + \zeta_{k\sigma}^2} + \bar{\gamma} \zeta_{k\sigma} \right] . \quad (6)$$

These results generalize previous analytical treatments²⁴ of cylindrical hole wires to the case with finite Zeeman splitting.

Inspection of the bulk dispersions in a finite magnetic field (Fig. 2) reveals an interesting cross-over behavior. At small k , i.e., small kinetic energy for motion perpendicular to the magnetic-field direction, a Zeeman splitting of HH and LH states with Landé factor in accordance with naive expectation ($g_{\text{HH}}^* = 6\kappa$ and $g_{\text{LH}}^* = 2\kappa$) is found. Evidently, these states have their spin closely aligned with the z axis. In contrast, at large k , the less-dispersive branches show no Zeeman splitting, while that of the more dispersive ones is characterized by g -factor 4κ . The latter situation is reminiscent of the Zeeman effect in 2D hole systems for an in-plane magnetic field.³

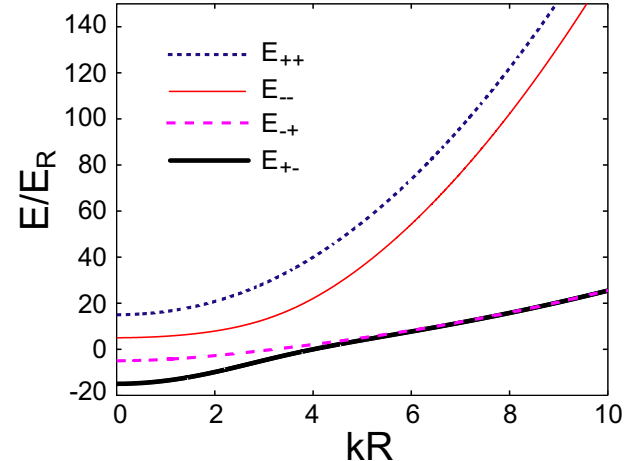


FIG. 2: (Color online) Energy dispersion $E_{\alpha\sigma}(k)$ of bulk-hole states that can be superimposed to form wire-subband bound states. Here R is an arbitrary length scale that will later be identified with the wire radius. The energy unit is $E_R = -\gamma_1 \hbar^2 / (2m_0 R^2)$, and a magnetic field $B = 10 \cdot \gamma_1 \hbar / (2\kappa e R^2)$ has been applied parallel to the z direction. The GaAs value $\bar{\gamma} = 0.37$ was assumed for the calculation.

TABLE I: Energies and effective g -factors for the lowest ten quasi-1D subband edges in a cylindrical hole wire. Units and parameters are the same as given in the caption of Fig. 1.

E/E_R	3.44	3.82	6.25	7.74	8.06	8.97	10.3	12.4	12.8	14.3
m	-2	-1	0	-3	-2	0	1	-4	-1	-3
g^*/κ	1.88	0.00	2.23	1.42	0.161	3.43	0.545	1.00	0.00	0.232

Hole-wire subband bound states are found by superimposing spinors $\psi_{k\alpha\sigma}m\alpha\sigma(r)$ with fixed m, σ and $E_{\alpha\sigma}(k_{\alpha\sigma}) = E$ to satisfy a hard-wall boundary condition at $r = R$. The resulting secular equation reads

$$a_+ J_m(k_+ R) J_{m+2}(k_- R) - a_- J_m(k_- R) J_{m+2}(k_+ R) = 0, \quad (7)$$

with conserved index σ suppressed for the sake of brevity. Solving Eq. (7) for E yields the subband energies $E_{nm\sigma}(B)$ for a cylindrical hole wire subject to a parallel magnetic field of magnitude B . In general, these are mixtures of the bulk states $\psi_{km\pm\sigma}$. Exceptions are states with $m = -1$, for which Eq. (7) specializes to the condition $J_1(k_{\pm}R) = 0$ that can be satisfied by the individual states $\psi_{km+\sigma}$ and $\psi_{km-\sigma}$. At finite B , levels $E_{nm\pm}$ are Zeeman-split. We calculate the corresponding g -factors using²⁵

$$g_{nm}^* = \lim_{B \rightarrow 0} \left| \frac{E_{nm+}(B) - E_{nm-}(B)}{\mu_B B} \right|. \quad (8)$$

Table I summarizes results obtained for the ten lowest wire subbands when the GaAs value for $\bar{\gamma}$ is assumed. The strong variation of g^* for different wire levels is illustrated in Fig. 1.

The first subband has g^* close to 2κ , as expected for a LH state with spin polarization parallel to the wire axis.²⁶ The second level belongs to the above-mentioned special class of states with $m = -1$, which are pure bulk states and therefore have g -factor equal to either 0 or 4κ . To obtain a fuller understanding of how various effective g -factor values for hole-wire subbands edges emerge, we analyze the corresponding bound states in terms of invariants for the spin-3/2 density matrix.

Spin polarization of hole-wire bound states. The peculiar physical properties of hole quantum wires can be attributed, in a very general way, to finite HH-LH mixing present even at the subband edges.²⁷ A quantitative characterization of the latter is typically attempted by considering expectation values for spin-3/2 projections on a fixed axis.^{18,20,27} In particular for a wire geometry, the usefulness of such an approach can be limited by ambiguities in the choice of a suitable projection axis. Hence, a characterization of hole states in terms of scalar invariants would be much more meaningful. In the following, we provide such an analysis in terms of a multipole expansion of spin-3/2 density matrices.⁸

As hole states are four-spinors, there exist four scalars ρ_0, \dots, ρ_3 to characterize their spin-3/2 density matrix. Here we adopted the notation of Ref. 8, where ρ_0 is proportional to the hole (charge) density, ρ_1 is a dipole moment related to the hole-spin polarization, the quadrupole moment ρ_2 quantifies HH-LH mixing, and ρ_3 is an octupole moment. It is an intriguing feature of spin-3/2 physics that magnetic fields can

induce a substantial octupole moment instead of a spin polarization (dipole moment) in 2D hole systems.⁸ Here we observe an analogous property of hole spin for individual states at the quasi-1D subband edges and relate our findings to the measurable g -factors of these states.

Within our model for a hole quantum wire, states at the subband edge are superpositions of HH and LH amplitudes corresponding to \hat{J}_z projection $\sigma 3/2$ and $-\sigma 1/2$, respectively. [See Eqs. (4).] For these wave functions, relations exist between the multipole invariants of the spin-3/2 density matrix:

$$\rho_0^2 = 2\rho_2^2 = \rho_1^2 + \rho_3^2. \quad (9)$$

The left equality in Eq. (9) quantifies the HH-LH mixing that is present in subband-edge states. The right equality in the same equation implies that, for each of these states, the magnitudes of spin polarization and octupole moment are complementary. In particular, a state with no spin polarization will have a maximum octupole moment and *vice versa*. We are thus able to fully characterize the spin properties of each subband-edge bound state by considering only ρ_1^2/ρ_0^2 . When derived from the radial part of the wire-subband wave function, this quantity provides a measure of local hole spin polarization. Figure 3 shows results for the five lowest cylindrical-wire subband edges. The (mainly) LH character of the lowest subband is apparent (ρ_1^2/ρ_0^2 is almost constant at 0.2), as is the vanishing of spin polarization for the next subband. Higher subbands show an evolving mixture of HH/LH character in their spin-polarization profile.

A comparison of spin-polarization profiles (Fig. 3) and effective g -factors (Table I) for each level yields a consistent picture. States with mainly LH (HH) character, i.e., those having $\rho_1^2/\rho_0^2 \approx 1/5$ (9/5) can be associated with a definite spin polarization parallel to the wire axis. Their corresponding g^* is close to the expected value 2κ (6κ). The lowest subband-edge state is an example for such a polarized (LH) state. Other

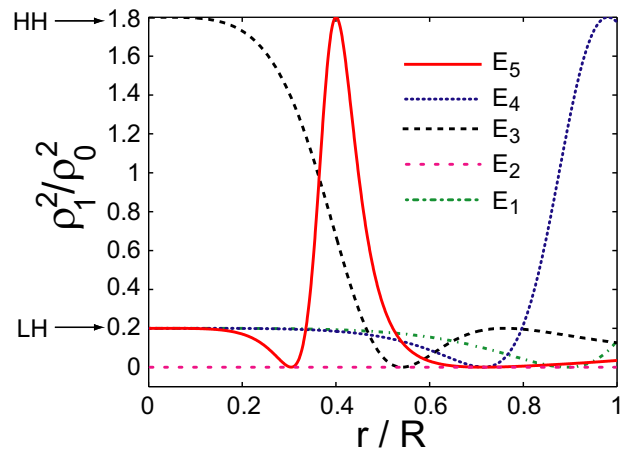


FIG. 3: (Color online) Radial profile of the (normalized squared magnitude of) local hole-spin polarization, calculated for the five lowest wire-subband-edge bound states. Pure HH (LH) states, defined by spin projection parallel to the z axis (i.e., the wire axis), have $\rho_1^2/\rho_0^2 = 9/5$ (1/5).

states exhibit a mixed spin-polarization profile, i.e., have both HH and LH polarizations present in different regions across the wire. The associated g -factor values can vary widely. Finally, states exist with vanishing hole-spin polarization over (most of) the wire cross-section. By virtue of Eq. (9), these states have a large spin-3/2 octupole moment. The second-lowest subband is an example for this class of states, whose g -factor turns out to be (close to) zero. The remarkable correspondence between local spin-polarization profiles and g -factor values for hole-wire levels is another example for intriguing spin physics emerging in nanostructures with strong spin-orbit coupling. The possibility to access individual properties of quasi-1D subband edges in transport experiments^{4,14} should enable the detailed study of hole states with large and small spin polarizations and spin octupole moments, respectively.

Principal caveats. To gauge the relevance of our results for real experiments, we need to discuss a few idealizations and approximations that are implicit in our model. Most importantly, we neglected orbital magnetic-field effects, band warping, and coupling to the conduction and split-off valence

bands. In addition, realistic wires will show deviations from perfect cylindrical symmetry and usually have a softer than hard-wall confinement.

In principle, any physical property affecting HH-LH mixing will quantitatively change g^* . It can be expected, however, that effects of band warping and remote bands are small, as they turned out to be for 2D hole systems.⁸ Cross-sectional shape of a hole wire generally affects its spin splitting.²⁶ However, a recent numerical study²⁰ found results for square CdTe wires that agree closely with those presented in this work. A detailed comparison with experiment will need to address orbital effects due to the typically not-so-small magnetic fields used to measure g^* .^{4,14,23} Interpretation of data obtained in hole point contacts⁴ also requires a better understanding of the transition region between 2D HH contacts and a constriction, and a proper treatment of the strong quantum-well and soft lateral confinements.

Acknowledgments. We thank P. Brusheim, A. Führer, M. Governale, A.R. Hamilton, R. Winkler, and H.Q. Xu for useful discussions. DC acknowledges support from the Massey University Research Fund.

¹ S. A. Wolf, D. D. Awschalom, R. A. Buhrmann, J. M. Daughton, S. von Molnár, M. L. Roukes, A. Y. Chtchelkanova, and D. M. Treger, *Science* **294**, 1488 (2001); D. D. Awschalom, D. Loss, and N. Samarth, eds., *Semiconductor Spintronics and Quantum Computation* (Springer, Berlin, 2002).

² S. A. Crooker and D. L. Smith, *Phys. Rev. Lett.* **94**, 236601 (2005); Y. K. Kato, R. C. Myers, A. C. Gossard, and D. D. Awschalom, *Appl. Phys. Lett.* **87**, 022503 (2005); D. Culcer, C. Lechner, and R. Winkler, *Phys. Rev. Lett.* **97**, 106601 (2006).

³ R. Winkler, *Spin-Orbit Coupling Effects in Two-Dimensional Electron and Hole Systems* (Springer, Berlin, 2003).

⁴ R. Danneau, O. Klochan, W. R. Clarke, L. H. Ho, A. P. Micolich, A. R. Hamilton, M. Y. Simmons, M. Pepper, D. Ritchie, and U. Zülicke, *Phys. Rev. Lett.* **97**, 026403 (2006).

⁵ C. E. Pryor and M. E. Flatté, *Phys. Rev. Lett.* **96**, 026804 (2006).

⁶ K.-M. Haendel, R. Winkler, U. Denker, O. G. Schmidt, and R. J. Haug, *Phys. Rev. Lett.* **96**, 086403 (2006).

⁷ R. M. Dreizler and E. K. U. Gross, *Density-Functional Theory* (Springer, Berlin, 1990).

⁸ R. Winkler, *Phys. Rev. B* **70**, 125301 (2004).

⁹ R. Winkler, *Phys. Rev. B* **71**, 113307 (2005).

¹⁰ J. M. Luttinger, *Phys. Rev.* **102**, 1030 (1956).

¹¹ K. Suzuki and J. C. Hensel, *Phys. Rev. B* **9**, 4184 (1974).

¹² H. W. van Kesteren, E. C. Cosman, W. A. J. A. van der Poel, and C. T. Foxon, *Phys. Rev. B* **41**, 5283 (1990).

¹³ S. Y. Lin, H. P. Wei, D. C. Tsui, J. F. Klem, and J. S. J. Allen, *Phys. Rev. B* **43**, 12110 (1991).

¹⁴ N. K. Patel, J. T. Nicholls, L. Martín-Moreno, M. Pepper, J. E. F. Frost, D. A. Ritchie, and G. A. C. Jones, *Phys. Rev. B* **44**, R10973 (1991).

¹⁵ W. Lu and C. M. Lieber, *J. Phys. D: Appl. Phys.* **39**, R387 (2006); L. Samuelson, *Mater. Today* **6**(10), 22 (2003).

¹⁶ L. N. Pfeiffer, R. de Picciotto, K. W. West, K. W. Baldwin, and C. H. L. Quay, *Appl. Phys. Lett.* **87**, 073111 (2005).

¹⁷ R. Danneau, W. R. Clarke, O. Klochan, A. P. Micolich, A. R. Hamilton, M. Y. Simmons, M. Pepper, and D. A. Ritchie, *Appl. Phys. Lett.* **88**, 012107 (2006).

¹⁸ F. V. Kyrychenko and J. Kossut, *Phys. Rev. B* **61**, 4449 (2000); S. Çakmak, A. M. Babayev, E. Artunç, A. Kökçe, and S. Çakmaktepe, *Physica E* **18**, 365 (2003).

¹⁹ X. W. Zhang, Y. H. Zhu, and J. B. Xia, *Eur. Phys. J. B* **52**, 133 (2006).

²⁰ Y. Harada, T. Kita, O. Wada, and H. Ando, *Phys. Rev. B* **74**, 245323 (2006).

²¹ N. O. Lipari and A. Baldereschi, *Phys. Rev. Lett.* **25**, 1660 (1970).

²² In real nanowires, certain subbands have additional extrema at finite p_z . See M. P. Persson and H. Q. Xu, *Nano Lett.* **4**, 2409 (2004); *Phys. Rev. B* **73**, 125346 (2006).

²³ Neglecting orbital magnetic-field effects is possible, e.g., in magnetic semiconductors that show a giant Zeeman effect [J. K. Furdyna, *J. Appl. Phys.* **64**, R29 (1988)].

²⁴ P. C. Sercel and K. J. Vahala, *Phys. Rev. B* **42**, 3690 (1990).

²⁵ Any two degenerate levels $E_{nm\pm}(0)$ are distinguished by quantum numbers $\pm(m + 3/2)$ of a new "total" angular momentum²⁴ $\hat{F}_z = \hat{J}_z - i\partial_\varphi$. Lifting of this degeneracy for finite B implies that these doublets are equivalent to spin-1/2 degrees of freedom with g -factor given by (8).

²⁶ U. Zülicke, *phys. stat. sol. (c)* **3**, 4354 (2006).

²⁷ G. Bastard, J. A. Brum, and R. Ferreira, in: *Solid State Physics*, vol. 44 (Academic Press, San Diego, 1991), pp. 229–415.